

Baseline Suvmax Correlates with Tumor Hypoxia and Patient Outcomes in Nasopharyngeal Carcinoma: Employing Transcriptomic Gene Signature Analysis

Jianming Ding

Department of Radiation Oncology, Clinical Oncology School of Fujian Medical University, Fujian Cancer Hospital

Qian Li

Department of Radiation Oncology, Clinical Oncology School of Fujian Medical University, Fujian Cancer Hospital

Yuhao Lin

Department of Radiation Oncology, Clinical Oncology School of Fujian Medical University, Fujian Cancer Hospital

Xiaobing Zheng

Department of Radiation Oncology, Clinical Oncology School of Fujian Medical University, Fujian Cancer Hospital

Chaoxiong Huang

Department of Radiation Oncology, Clinical Oncology School of Fujian Medical University, Fujian Cancer Hospital

Jiabiao Hong

Department of Radiation Oncology, Clinical Oncology School of Fujian Medical University, Fujian Cancer Hospital

Zhaodong Fei (✉ feizhaodong@fjmu.edu.cn)

Department of Radiation Oncology, Clinical Oncology School of Fujian Medical University, Fujian Cancer Hospital

Chuanben Chen

Department of Radiation Oncology, Clinical Oncology School of Fujian Medical University, Fujian Cancer Hospital

Article

Keywords: suvmax, glucose metabolism gene, patient prognosis, hypoxia

Posted Date: January 16th, 2024

DOI: <https://doi.org/10.21203/rs.3.rs-3848296/v1>

License:  This work is licensed under a Creative Commons Attribution 4.0 International License.

[Read Full License](#)

Additional Declarations: No competing interests reported.

Abstract

Objective: To assess the prognostic relevance of the maximum standard uptake value (Suvmax) in Nasopharyngeal carcinoma (NPC), establish a gene signature correlated with Suvmax and explore the potential biological mechanisms underlying these associations for predicting clinical outcomes.

Methods: A cohort of 726 NPC patients underwent analysis to determine correlations between Suvmax and various clinical variables, including tumor stage, metabolic tumor volume (MTV), and lactate dehydrogenase (LDH) levels. RNA sequencing data was utilized to identify genes related to Suvmax, which were then used to develop a 'Suv-signature'. Additionally, transcriptome enrichment analysis was conducted to investigate the potential biological mechanisms underlying the observed correlations.

Results: Higher Suvmax values were associated with increased tumor burden and worse prognosis. The 'Suv-signature' consisting of 10 genes, showed a positive correlation with Suvmax and predicted poorer survival outcomes. This signature was highly expressed in malignant epithelial cells and was associated with hypoxia and resistance to radiotherapy. Additionally, the signature showed a negative correlation with immune function.

Conclusion: Suvmax is a valuable prognostic indicator in NPC, with higher values predicting worse outcomes. The 'Suv-signature' offers further prognostic insights, linking glucose metabolism to tumor aggressiveness, treatment resistance, and immune function, and may serve as a potential biomarker for NPC.

Introduction

Nasopharyngeal carcinoma (NPC), arising from the mucosal epithelium of the nasopharynx, poses a significant challenge due to its aggressiveness and distinctive anatomical location^[1]. The primary treatment modality for NPC is radiotherapy, particularly with the advancements brought about by intensity-modulated radiation therapy (IMRT)^[2]. While IMRT has significantly improved the 5-year overall survival rate, recurrent and distant metastatic NPC remains a therapeutic challenge^[3]. Identifying effective biomarkers is crucial for predicting clinical outcomes and tailoring individualized treatments to enhance overall prognosis.

F18-FDG PET/CT, a functional imaging modality allowing quantitative assessment of glucose uptake, plays a crucial role in NPC diagnosis and staging^[4]. Notably, the maximum standard uptake value (Suvmax) derived from F18-FDG PET/CT has demonstrated predictive capabilities for survival outcomes in various malignancies^[5, 6]. Studies consistently highlight Suvmax as a significant predictor of clinical prognosis in NPC^[4, 7]. Research suggests a negative correlation between Suvmax and the expression of fructose-1,6-diphosphatase 1 (FBP 1), indicating Suvmax's potential role as a prognostic indicator through mechanisms associated with glucose metabolism^[5]. However, the detailed exploration of glucose metabolism genes at the transcriptome level remains limited.

This study aims to identify significant glucose metabolism genes associated with Suvmax using RNA sequencing datasets and formulate a gene marker, termed the "Suv-signature." Additionally, the investigation delves into the mechanism by which Suvmax predicts prognosis through enrichment analysis.

Materials and Methods

Patients

This retrospective study included 726 newly diagnosed individuals with nasopharyngeal carcinoma (NPC) who underwent complete treatment at our center between January 2012 and December 2018. Inclusion criteria were as follows: a) confirmation of primary NPC through biopsy; b) availability of comprehensive baseline clinical data; c) pre-treatment whole-body 18F-FDG PET/CT; d) receipt of radical treatment. Exclusion criteria comprised: a) Suvmax of the primary tumor less than 2.5; b) presence of distant metastasis; c) concurrent other malignancies; d) coexistence with a fatal disease; e) history of cancer treatment; f) insufficient follow-up data and image information. All patients underwent restaging according to the 8th edition of the AJCC/TNM staging system. The study was conducted in compliance with the Helsinki Declaration, and the Ethics Committee of Fujian Cancer Hospital approved this research.

FDG PET / CT imaging

The Gemini TF 64 PET/CT scanner (Philips, The Netherlands) was employed for the studies. Prior to the injection of 18F-FDG, all patients observed a fasting period of more than 6 hours, and their serum glucose levels were maintained between 3.9 and 6.5 mmol/L. Subsequently, 18F-FDG was intravenously administered at doses ranging from 148 to 296 MBq. Following injection, patients rested for 60 minutes in a dimly lit room. CT scans were then acquired for all patients, covering from the head to the proximal thigh (140 kV; 2.5 mA; matrix 512×512; and scan slice thickness 4 mm). The recorded parameters included the Suvmax and MTV of the primary lesion, with MTV defined as the volume of the region with an SUV greater than 2.5.

Treatment and follow-up

A total of 682 patients (93.9% of the initial 726) underwent platinum-based chemotherapy. Within the entire cohort, 624 (86%), 532 (73.3%), and 162 (22.3%) cases received neoadjuvant, concurrent, and adjuvant chemotherapy, respectively. The predominant regimen employed was platinum in combination with paclitaxel or gemcitabine. Radiotherapy was conducted using intensity-modulated radiotherapy (IMRT), and the target volume and radiotherapy dose adhered to a previously established protocol^[8]. The prescribed radiotherapy doses were as follows: GTV:70 ~ 72.6Gy/31 ~ 33fx, CTV1:62 ~ 62.7Gy/31 ~ 33fx, and CTV2:54.4 ~ 56.2Gy/31 ~ 33

Local Recurrence-Free Survival (LRFS) was defined as the duration from pathological diagnosis to local relapse or the conclusion of the follow-up period. Distant Metastasis-Free Survival (DMFS) denoted the

duration a patient could survive without cancer spreading from the primary tumor to distant organs. Progression-Free Survival (PFS) was characterized as the interval from pathological diagnosis to the progression of tumor development or death. Overall Survival (OS) is defined as the period from the pathological diagnosis to the time when the patient succumbs to any cause. All patients adhered to a regular follow-up schedule, with assessments every 3 months for the first 2 years, every 6 months for years 3–5, and subsequently on an annual basis.

Acquisition and processing of RNA-seq data

Additional 29 tissue samples were obtained from NPC patients before treatment (Supplementary information, Table S1). RNA-seq experiment was performed at Geneplus-Beijing (Beijing, China). Tissues were subjected to total RNA isolation using a commercial RNA extraction kit. After whole transcriptome amplification, library construction was performed. Library quality analysis was performed using Aligent 2100 DNA 1000 Kit. Samples were sequenced using the DNBSEQ-T7 platform.

We used NPC gene expression profile GSE102349 with prognostic data to verify SUV-signature prognostic ability, because there was no external NPC transcriptome dataset with SUV information, we used the dataset of GSE135565 of breast cancer to verify whether SUV signature represents Suvmax, and the NPC single cell dataset used GSE150430. These data were downloaded from the GEO (<https://www.ncbi.nlm.nih.gov/geo/>) for the database.

Construction of the SUV-signature model

Relevant genes encoding glucose metabolism proteins were selected from the Molecular Features database (mSigDB). A total of 326 genes were manually curated into the glucose metabolism gene sets for further transcriptomic analysis (Supplementary information, Table S2). In order to make the results more representative, among the 29 patients who underwent transcriptome sequencing, the transcriptome data of the 8 patients with the lowest Suvmax and the 8 patients with the highest Suvmax were selected for analysis. Through Pearson correlation analysis of glucose metabolism gene set and Suvmax, all related genes ($p < 0.05$) were defined as Suvmax-related glucose metabolism genes, and 55 genes were selected for subsequent analysis (Supplementary information, Table S3). The selected Suvmax-related glucose metabolism genes were modeled by lasso-logistics, 10-fold cross-validation was carried out, lambda of the model with the lowest average cross-validation error was taken, coef coefficients were extracted and added to obtain the transcriptome tag of Suvmax, which was defined as SUV-signature.

The single-cell RNA-seq analysis

Single-cell mRNA-seq data have been reported by Yu-Pei Chen et al^[9]. The Python package Scanpy (version 1.4.6) was used to analyze these dataset. Clustering was performed using the UMAP algorithm. SUV-signature was calculated for each single cell. We then annotated the clusters following major cell types: B cells, epithelial cells, T cells, myeloid cells, NK cells and plasma cells. The SUV-signature of each class of cells was compared. T cells were divided into high score group and low score group

according to the median value of suv-signature, and the expression of HAVCR2, PDCD1, LAG3 and TIGIT in different groups were compared.

Differential gene analysis and Functional enrichment analysis

We conducted differential expression analysis on the groups categorized as high and low SUV based on the median Suvmax using the Lima package. Characteristics meeting the criteria of $|\log_2FC| > 2$ and $\text{adj.P} < 0.05$ were designated as differential expression features. Subsequently, hub genes underwent Gene Ontology (GO) and Kyoto Encyclopedia of Genes and Genomes (KEGG) enrichment analysis, facilitated by the cluster profile package^[10]. Furthermore, gene set enrichment analysis (GSEA) was executed on the gene expression matrix using the clusterProfiler package^[11].

Hypoxic score and Immune function analysis

We selected a 15-gene expression signature (ACOT7, ADM, ALDOA, CDKN3, ENO1, LDHA, MIF, MRPS17, NDRG1, P4HA1, PGAM1, SLC2A1, TPI1, TUBB6 and VEGFA) that has been shown to perform the best when classifying hypoxia status^[12]. The hypoxia score for each tumor sample was calculated by using gene set variation analysis (GSVA) based on 15 mRNA-based hypoxia signatures. The immune scores, stromal scores, estimate scores, and tumor purity in the study were calculated using the ESTIMATE algorithm. Then Pearson correlation analysis was applied to the relationship between these indicators and suv signature in our center data and the GSE102349 dataset. The Pearson correlation coefficient R value is calculated.

Statistical analysis

R software (version 3.6.1) and Python software (version 3.10) were used to organize, analyze and visualize relevant data. We used KM curves, log rank test to assess survival data between different risk groups. Two-sample t-test was used for comparison between groups and correlation between groups by Spearman rank correlation or Pearson correlation. Test levels were considered statistically significant at $P < 0.05$.

Ethics approval and Consent to participate

The study was approved by the Ethical Committee of Fujian Cancer Hospital (YKT2020-011-01) and was in accordance with the 1964 Helsinki declaration and its later amendments or comparable ethical standards. Patient identifiers such as names were not collected, instead patients were given a numerical identifier. Informed consent was obtained from all participants and for those under 18 years, from a parent or legal guardian. For confidentiality, the patients' charts were used only within the confines of the records department and only the investigators and study assistant had access to the files.

Results

Higher Suvmax values suggest a larger tumor burden and poor prognosis

In this study, the median follow-up duration was 49.0 months (range: 3.0-118.0 months). The median age of patients was 47 years (range: 11.0-78.0 years), and the majority of patients presented with AJCC stages III (43.4%) and IV (37.1%). Patient characteristics are summarized in Table 1. Throughout the follow-up period, 63 (8.7%) experienced local failure, 88 (12.1%) experienced distant metastasis, 161 (22.2%) encountered disease progression, and 75 (10.3%) succumbed to mortality. The 5-year rates for Local Recurrence-Free Survival (LRFS), Distant Metastasis-Free Survival (DMFS), Progression-Free Survival (PFS), and Overall Survival (OS) were 89.7%, 87.7%, 76.7%, and 87.8%, respectively.

The correlation between Suvmax and clinical variables was examined. Suvmax demonstrated associations with T stage ($P < 0.01$, Figure 1A), MTV ($r=0.691$, $P < 0.001$, Figure 1C), and LDH ($r=0.178$, $P < 0.001$, Figure 1D). Suvmax exhibited limited correlation with N-stage (Figure 1B). Subsequently, a survival analysis was conducted. The ROC curve determined the optimal cutoff value for Suvmax to predict overall survival, maximizing Youden's index. Patients were then categorized into high and low Suvmax groups. The results revealed that LRFS (HR=0.42; $P=0.003$, Figure 1E), PFS (HR=0.71; $P=0.036$, Figure 1G), and OS (HR=0.50; $P=0.007$, Figure 1H) in patients with high Suvmax were all significantly lower than those in patients with low Suvmax. Unexpectedly, there was no significant difference in DMFS between patients with high Suvmax and those with low Suvmax ($P=0.318$, Figure 1F).

The SUV-signature was formulated utilizing genes associated with glucose metabolism.

In a cohort of 29 patients undergoing transcriptome sequencing, individuals were categorized into two groups based on the median value of Suvmax. Differential gene analysis (Figure 2A), Gene Ontology (GO) analysis (Figure 2B), and Gene Set Enrichment Analysis (GSEA) (Figure 2C) revealed the enrichment of Suvmax differential genes in pathways related to glucose metabolism. Consequently, we explored the construction of the Suv-signature using genes associated with glucose metabolism.

Through correlation analysis between genes related to glucose metabolism and Suvmax, we identified 55 genes associated with glucose metabolism. Lasso-logistics modeling (Figure 2D and 2E) was conducted with 10-fold cross-validation, and the lambda value (0.00392) corresponding to the model with the smallest cross-validation mean error was selected. The coef coefficients were then extracted and combined to derive the Suv-signature (Figure 2F). The formulated formula is as follows: Suv-signature = $0.007 * PKM + 0.375 * SEH1L - 0.44 * LHPP + 0.007 * LDHA + 3.713 * PPFIA4 + 0.015 * PFKFKB3 - 0.099 * MPI - 11.022 * ZBTB20 - 0.672 * CLDN9 + 3.186 * PGAM4$.

Verify whether Suv-signature can predict Suvmax and poor prgonosis

In order to prove that Suv-signature model can predict Suvmax, correlation analysis was conducted between Suv-signature and Suvmax using our dataset of 16 cases and 29 cases (Figure3A and FigureS1) and GSE135565 dataset (Figure3B). Suv-signature was found to be positively correlated with Suvmax, which proved that Suv-signature could represent Suvmax. Meanwhile, we conducted a prognosis validation using the GSE102349 dataset and stratified the cohorts based on the median Suv-signature

values. Our findings revealed a significantly poorer prognosis in the high Suv-signature group compared to the low Suv-signature group. (P=0.006, Figure3C).

Subsequently, we utilized the single-cell RNA sequencing dataset (GSE150430) from NPC to investigate the intrinsic biological characteristics of Suvmax. Employing UMAP, we categorized the cells into six clusters, encompassing B cells, T cells, NK cells, myeloid cells, plasma cells, and epithelial cells (Figure 3D). SUV-signature scores were then computed across these distinct clusters, revealing the highest expression in epithelial tissues (Figure 3E). Further delineating epithelial cells into malignant and normal subtypes, we observed a significantly elevated Suv-signature expression in malignant epithelial cells compared to their non-malignant counterparts (Figures 3F-3I).

Suv-signature was associated with hypoxic and radiotherapy resistance

A correlation analysis was conducted on our center's dataset (Figure 4A) and the GSE102349 dataset (Figure 4D) to examine the relationship between Suv-signature and hypoxia score. The results revealed a significant correlation, with an R value of 0.76 in our center dataset and 0.62 in the GSE102349 dataset, indicating a close association between Suv-signature and hypoxia score. The outcomes from the Gene Set Enrichment Analysis (GSEA) further validate the enrichment of Suv-signature within hypoxia-associated hallmarks, as illustrated in Figure 4B and 4E. This observation supports the notion that Suv-signature could potentially serve as an indicator of hypoxia.

Additionally, our investigation revealed a notable enrichment score for Suv-signature within the radiotherapy (RT) resistance gene set, as depicted in Figure 4C and 4F. Given that radiotherapy stands as the primary treatment for NPC, and its insensitivity implies a poor prognosis, the connection between Suv-signature and RT resistance becomes pivotal. Notably, hypoxia serves as a known mechanism contributing to radiotherapy resistance. This implies that Suvmax may potentially predict an unfavorable prognosis by influencing radiotherapy sensitivity through oxygen deficiency.

SUV-signature was associated with immune function

In the single-cell RNA dataset, T cells were stratified into high and low Suv-signature groups based on the median values of Suv-signature. Our observations revealed a significant upregulation of immunosuppressive markers, including HAVCR2, PDCD1, LAG3, and TIGIT, in T cells exhibiting high Suv-signature scores (Figure 5A-D).

Expanding our analysis to the GSE102349 cohort, we further explored the association between Suv-signature and immune score, stromal score, predicted score, and tumor purity (Figure 5E-H). Remarkably, we found a negative correlation between Suv-signature and immune score, stromal score, and predicted score, while a positive correlation was observed with tumor purity. These findings suggest an inverse relationship between Suv-signature and immune function.

Discussion

In this study, our focus on genes associated with glucose metabolism enabled the formulation of transcriptomic signatures linked to Suvmax in NPC patients. To the best of our knowledge, our study is the first to delineate the transcriptomic profile of glucose uptake, assess its prognostic value, and explore underlying mechanisms in individuals with NPC. The findings underscored that patients with a high Suv-signature score faced an unfavorable prognosis. Delving into biological mechanisms, we established that the SUV-signature could function as an indicator of hypoxia, suggesting a plausible association between elevated Suv levels and hypoxia-induced phenomena in NPC patients, such as radiotherapy resistance and immunosuppression. These insights contribute to a better understanding of the prognostic landscape and potential therapeutic targets in NPC.

The well-established Warburg effect posits that cancer cells preferentially metabolize glucose through glycolysis rather than more efficient mitochondrial oxidative phosphorylation, even under conditions of ample oxygen. FDG PET/CT capitalizes on increased glucose uptake precisely for tumor detection^[13]. Notably, studies have identified substantial differences in the expression of glucose uptake-dependent transporters in individuals with high and low Suvmax in HCC patients^[5]. Therefore, employing the gene expression associated with glucose metabolism to predict NPC prognosis emerges as a potentially valuable tool for precisely stratifying risk groups. In this study, we focused on ten glucose metabolism-related genes associated with Suvmax in NPC: PKM, SEH1L, LHPP, LDHA, PPFIA4, PFKFB3, MPI, ZBTB20, CLDN 9, and PGAM 4. The encoded pyruvate kinase from the PKM gene crucially regulates cellular metabolism by converting phosphoenolpyruvate (PEP) into pyruvate in glycolysis^[14]. SEH1L encodes a protein integral to the Nup107-160 nuclear pore complex, impacting cell growth and proliferation^[15]. LHPP encodes proteins participating in phosphorylation metabolism with anticancer effects^[16]. LDHA-encoded proteins, part of the lactate dehydrogenase family, are frequently overexpressed in cancer, promoting glycolysis and cancer progression^[17]. PPFIA4 encodes the Liprin- α 4 protein, associated with abnormal metabolic processes. Silencing PPFIA4 has been found to attenuate glycolysis, regulate glycolysis-related genes (PFKFB3 and ENO2), and inhibit cancer cell proliferation, migration, and invasion^[18]. The encoded phosphomannose isomerase by MPI plays a vital role in glycosylation reactions^[19]. ZBTB20, a transcriptional repressor, influences neurogenesis, glucose, and lipid metabolism. ZBTB20 induces ChREBP-A promoter transcriptional activity, regulating glycolytic and lipogenic enzyme genes and affecting glycolipid metabolism^[20]. CLDN 9 has been correlated with glycolytic levels in endometrial carcinoma and esophageal adenocarcinoma^[21]. PGAM, encoding proteins catalyzing the reversible reaction of 3-phosphoglycerate (3-PGA) to 2-phosphoglycerate (2-PGA) in the glycolysis pathway, regulates metabolism and energy production^[22].

The prognostic model incorporating these genes, termed Suv-signature, demonstrated robust stratification of Progression-Free Survival (PFS). The Suv-signature may hold significant implications for individualized precision therapy. Furthermore, our exploration into the cellular biology associated with Suv-signatures, utilizing single-cell RNA-seq data, revealed that malignant epithelial tissues exhibited the highest Suv-signature expression. This aligns with findings from Jin Meng^[6], supporting the notion of increased F18-FDG uptake by tumor cells. The Suvmax is relevant to various factors such as tumor

metabolic activity, tumor cell concentration, serum glucose level, and fat content. In parallel with these considerations, our study uncovered associations between Suvmax and MTV, LDH, and T stage. MTV and LDH, reflective of tumor burden [23], suggested that Suvmax is linked to tumor burden. T stage, indicative of the biological aggressiveness of tumors, further supported the association between Suvmax and the biological aggressiveness of NPC. Previous studies have also indicated the clinical prognostic value of Suvmax in NPC [7, 24]. For instance, in a study involving 253 patients with newly diagnosed metastatic NPC, those with higher Suvmax exhibited lower 3-year Overall Survival (OS) [7]. Consistent with these findings, our survival analysis demonstrated that patients with high Suvmax experienced worse OS, Progression Free Survival (PFS), and Local Recurrence-Free Survival (LRFS) compared to patients with low Suvmax. Simultaneously, the transcriptome signature representing Suvmax, constructed in our study, also indicated poor PFS, underscoring the prognostic significance of Suvmax in NPC. The ability of Suvmax to predict distant metastasis remains a topic of debate. While Meryem Aktan et al. identified Suvmax as an important prognostic factor for distant metastasis and its utility in evaluating Disease Free Survival (DFS) results [24], Kazuhiro Kitajima et al. found no significant correlation between primary tumor Suvmax and Distant Metastasis Free Survival (DMFS) [25]. Our study aligns with the latter, indicating that Suvmax may predict prognosis more through local treatment failure than distant metastasis.

Several studies have delved into the association between SUVmax or its related genomic features and radiosensitivity in various malignancies [6, 26]. Recently, there's emerging evidence that radiomics characteristics derived from PET/CT imaging, in combination with clinical parameters, hold promise for accurate therapeutic effect evaluation in NPC [27]. The potential of PET/CT to predict radiosensitivity was further demonstrated in an NPC xenograft nude mouse model [28]. Consistent with these findings, our enrichment analysis demonstrated an enrichment of gene sets associated with radiotherapy resistance in the high Suvsignature score group. Given that radiotherapy stands as the primary treatment for NPC, a high SUV-signature score in our study suggests that nasopharyngeal carcinoma may not be sensitive to radiotherapy, implying a poor prognosis. Additionally, both correlation analysis and enrichment analysis in our study highlighted a close relationship between SUV-signature and hypoxia. This aligns with prior reports indicating a hypoxia gene signature association with FDG uptake in liver and *lung* cancers [5, 29]. It is plausible that byproducts of glycolysis drive crucial biosynthetic pathways, providing a selective advantage to rapidly dividing cancer cells, and hypoxia signaling confers a survival advantage to tumor cells in a normoxic environment [30]. Studies have also shown that tumor hypoxia leads to radiotherapy resistance, primarily dependent on the generation of reactive oxygen species (ROS) and the formation of irreparable DNA damage resulting from peroxidation events [31]. Therefore, SUVmax emerges as a potential biomarker of hypoxia, influencing radiotherapy sensitivity and serving as a predictor of poor prognosis.

Moreover, in a study involving 84 NPC patients, Suvmax exhibited a positive correlation with PD-L1 expression in tumor cells and a negative correlation with PD-L1 expression in tumor-infiltrating immune cells [32]. A phase 1/2 trial similarly identified T cells within neoplastic lesions as pivotal mediators of

immunotherapy, assessable through whole-body PET imaging^[33]. In alignment with these investigations, our cohort also revealed a significant upregulation of immunosuppressive markers in T cells with high SUV-signature scores. The correlation between Suvmax and immunosuppression may be mediated through the effects of hypoxia. Hypoxia has been shown to impact immune function through hypoxia-induced factor-1 (HIF-1)^[34]. Immunosuppressive cells under hypoxic conditions can utilize fatty acid oxidation for cellular energy, maintaining immunosuppressive capabilities against effector T cells^[35]. Consequently, SUV-signature may serve as a tool to characterize the tumor immune microenvironment and potentially guide the use of immunosuppressive agents.

However, our study has several limitations. Firstly, the small sample size of patients undergoing transcriptomic sequencing for nasopharyngeal cancer, coupled with the absence of external transcriptomic data on Suvmax in this context, prompted us to perform external validation using breast cancer data. As such, the accuracy and reliability of the SUV-signature necessitate further confirmation through larger cohort studies with dedicated nasopharyngeal cancer datasets. Secondly, the retrospective nature of our study introduces the possibility of bias, underscoring the need for prospective studies to mitigate potential biases and enhance the robustness of our findings. Thirdly, while our bioinformatics analysis suggests that Suvmax may serve as a marker of hypoxia, the sensitivity and specificity of Suvmax in this role remain unclear. Rigorous studies with well-defined methodologies are essential to clarify the utility of Suvmax as a marker of hypoxia, shedding light on its potential diagnostic accuracy.

In summary, our study highlights the utility of Suvmax as a predictive indicator for poor prognosis in NPC. The development of a Suvmax based transcriptomic signature underscores its potential as a marker for predicting tumor hypoxia. Furthermore, our findings suggest that the biological behavior associated with Suvmax may contribute to a diminished prognosis by impacting radiation sensitivity and suppressing immune function. These insights offer valuable perspectives for understanding the clinical implications of Suvmax in NPC and may guide future therapeutic strategies.

Declarations

Author contribution:

Study concept and design: CB C, ZD F. Acquisition, analysis, or interpretation of data: All authors. Drafting of the manuscript: JM D, LQ. Critical revision of the manuscript for important intellectual content: All authors. Statistical analysis: YH L, XB Z, CX H, JB H. Study supervision: CB C, ZD F.

Funding: This work was supported by research projects for the Bethune-Translational Medicine Research Fund for Oncology radiotherapy (flzh202126).

Conflicts of interest statement: The authors declare that they have no competing interests.

Data availability statement:

The datasets generated or analyzed during the study are available from the corresponding author on reasonable request.

Ethics approval and Consent to participate: The study was approved by the Ethical Committee of Fujian Cancer Hospital (YKT2020-011-01) and was in accordance with the 1964 Helsinki declaration and its later amendments or comparable ethical standards. Patient identifiers such as names were not collected, instead patients were given a numerical identifier. Informed consent was obtained from all participants and for those under 18 years, from a parent or legal guardian. For confidentiality, the patients' charts were used only within the confines of the records department and only the investigators and study assistant had access to the files.

References

1. Chen YP, Chan ATC, Le QT, Blanchard P, Sun Y, Ma J. Nasopharyngeal carcinoma. *Lancet*. 2019;394(10192):64–80.
2. Wong KCW, Hui EP, Lo KW, et al. Nasopharyngeal carcinoma: an evolving paradigm. *Nat Rev Clin Oncol*. 2021;18(11):679–695.
3. Zhang L, Huang Y, Hong S, et al. Gemcitabine plus cisplatin versus fluorouracil plus cisplatin in recurrent or metastatic nasopharyngeal carcinoma: a multicentre, randomised, open-label, phase 3 trial [published correction appears in *Lancet*. 2016;388(10054):1882]. *Lancet*. 2016;388(10054):1883–1892.
4. Sanli Y, Zukotynski K, Mitra E, et al. Update 2018: 18F-FDG PET/CT and PET/MRI in Head and Neck Cancer. *Clin Nucl Med*. 2018;43(12):e439-e452.
5. Xia H, Chen J, Gao H, et al. Hypoxia-induced modulation of glucose transporter expression impacts 18F-fluorodeoxyglucose PET-CT imaging in hepatocellular carcinoma. *Eur J Nucl Med Mol Imaging*. 2020;47(4):787–797.
6. Meng J, Deshayes E, Zhang L, et al. Prognostic value of metabolic signature on 18F-FDG uptake in breast cancer patients after radiotherapy. *Mol Ther Oncolytics*. 2021;23:412–419. Published 2021 Oct 28.
7. Sun XS, Liang YJ, Liu SL, et al. Maximal standard uptake values of 18F-fluoro-2-deoxy-D-glucose positron emission tomography compared with Epstein-Barr virus DNA as prognostic indicators in de novo metastatic nasopharyngeal carcinoma patients. *BMC Cancer*. 2019;19(1):908. Published 2019 Sep 11.
8. Lin S, Pan J, Han L, et al. Update report of nasopharyngeal carcinoma treated with reduced-volume intensity-modulated radiation therapy and hypothesis of the optimal margin. *Radiother Oncol*. 2014;110(3):385–389.
9. Chen YP, Yin JH, Li WF, et al. Single-cell transcriptomics reveals regulators underlying immune cell diversity and immune subtypes associated with prognosis in nasopharyngeal carcinoma. *Cell Res*. 2020;30(11):1024–1042.

10. Yu G, Wang LG, Han Y, He QY. clusterProfiler: an R package for comparing biological themes among gene clusters. *OMICS*. 2012;16(5):284–287.
11. Hänzelmann S, Castelo R, Guinney J. GSEA: gene set variation analysis for microarray and RNA-seq data. *BMC Bioinformatics*. 2013;14:7. Published 2013 Jan 16.
12. Ye Y, Hu Q, Chen H, et al. Characterization of Hypoxia-associated Molecular Features to Aid Hypoxia-Targeted Therapy. *Nat Metab*. 2019;1(4):431–444.
13. Hsu PP, Sabatini DM. Cancer cell metabolism: Warburg and beyond. *Cell*. 2008;134(5):703–707.
14. Morita M, Sato T, Nomura M, et al. PKM1 Confers Metabolic Advantages and Promotes Cell-Autonomous Tumor Cell Growth. *Cancer Cell*. 2018;33(3):355–367.e7.
15. Platani M, Samejima I, Samejima K, Kanemaki MT, Earnshaw WC. Seh1 targets GATOR2 and Nup153 to mitotic chromosomes. *J Cell Sci*. 2018;131(9):jcs213140. Published 2018 May 1.
16. Hindupur SK, Colombi M, Fuhs SR, et al. The protein histidine phosphatase LHPP is a tumour suppressor. *Nature*. 2018;555(7698):678–682.
17. Liu J, Zhang C, Zhang T, et al. Metabolic enzyme LDHA activates Rac1 GTPase as a noncanonical mechanism to promote cancer. *Nat Metab*. 2022;4(12):1830–1846.
18. Huang J, Yang M, Liu Z, et al. PPFIA4 Promotes Colon Cancer Cell Proliferation and Migration by Enhancing Tumor Glycolysis. *Front Oncol*. 2021;11:653200. Published 2021 May 20.
19. Ichikawa M, Scott DA, Losfeld ME, Freeze HH. The metabolic origins of mannose in glycoproteins. *J Biol Chem*. 2014;289(10):6751–6761.
20. Xie Z, Ma XH, Bai QF, et al. ZBTB20 is essential for cochlear maturation and hearing in mice. *Proc Natl Acad Sci U S A*. 2023;120(24):e2220867120.
21. Wang ZH, Zhang YZ, Wang YS, Ma XX. Identification of novel cell glycolysis related gene signature predicting survival in patients with endometrial cancer. *Cancer Cell Int*. 2019;19:296. Published 2019 Nov 14.
22. Fukushi A, Kim HD, Chang YC, Kim CH. Revisited Metabolic Control and Reprogramming Cancers by Means of the Warburg Effect in Tumor Cells. *Int J Mol Sci*. 2022;23(17):10037. Published 2022 Sep 2.
23. Cottreau AS, Meignan M, Nioche C, et al. Risk stratification in diffuse large B-cell lymphoma using lesion dissemination and metabolic tumor burden calculated from baseline PET/CT†. *Ann Oncol*. 2021;32(3):404–411.
24. Aktan M, Kanyilmaz G, Yavuz BB, Koc M, Eryilmaz MA, Adli M. Prognostic value of pre-treatment 18F-FDG PET uptake for nasopharyngeal carcinoma. *Radiol Med*. Published online November 25, 2017.
25. Kitajima K, Suenaga Y, Kanda T, et al. Prognostic value of FDG PET imaging in patients with laryngeal cancer. *PLoS One*. 2014;9(5):e96999. Published 2014 May 12.
26. Na F, Wang J, Li C, Deng L, Xue J, Lu Y. Primary tumor standardized uptake value measured on F18-Fluorodeoxyglucose positron emission tomography is of prediction value for survival and local

- control in non-small-cell lung cancer receiving radiotherapy: meta-analysis. *J Thorac Oncol*. 2014;9(6):834–842.
27. Kim SJ, Choi JY, Ahn YC, Ahn MJ, Moon SH. The prognostic value of radiomic features from pre- and post-treatment 18F-FDG PET imaging in patients with nasopharyngeal carcinoma. *Sci Rep*. 2023;13(1):8462. Published 2023 May 25.
 28. Zheng Y, Yang Z, Zhang Y, et al. The preliminary study of 18F-FLT micro-PET/CT in predicting radiosensitivity of human nasopharyngeal carcinoma xenografts. *Ann Nucl Med*. 2015;29(1):29–36.
 29. Heiden BT, Chen G, Hermann M, et al. 18F-FDG PET intensity correlates with a hypoxic gene signature and other oncogenic abnormalities in operable non-small cell lung cancer. *PLoS One*. 2018;13(7):e0199970. Published 2018 Jul 2.
 30. Vander Heiden MG, Cantley LC, Thompson CB. Understanding the Warburg effect: the metabolic requirements of cell proliferation. *Science*. 2009;324(5930):1029–1033.
 31. Graham K, Unger E. Overcoming tumor hypoxia as a barrier to radiotherapy, chemotherapy and immunotherapy in cancer treatment. *Int J Nanomedicine*. 2018;13:6049–6058. Published 2018 Oct 4.
 32. Zhao L, Zhuang Y, Fu K, et al. Usefulness of [18F]fluorodeoxyglucose PET/CT for evaluating the PD-L1 status in nasopharyngeal carcinoma. *Eur J Nucl Med Mol Imaging*. 2020;47(5):1065–1074.
 33. Kist de Ruijter L, van de Donk PP, Hooiveld-Noeken JS, et al. Whole-body CD8 + T cell visualization before and during cancer immunotherapy: a phase 1/2 trial. *Nat Med*. 2022;28(12):2601–2610.
 34. Kheshtchin N, Hadjati J. Targeting hypoxia and hypoxia-inducible factor-1 in the tumor microenvironment for optimal cancer immunotherapy. *J Cell Physiol*. 2022;237(2):1285–1298.
 35. Bader JE, Voss K, Rathmell JC. Targeting Metabolism to Improve the Tumor Microenvironment for Cancer Immunotherapy. *Mol Cell*. 2020;78(6):1019–1033.

Tables

Table 1
Clinical characteristics of patients

Characteristic	Overall
Total patients	726
Gender, n (%)	
Male	527 (72.6)
Female	199 (27.4)
T stage, n (%)	
T1	171 (23.5)
T2	150 (20.7)
T3	271 (37.3)
T4	134 (18.5)
N stage, n (%)	
N0	91 (12.5)
N1	250 (34.4)
N2	233 (32.1)
N3	152 (20.9%)
TNM stage, n (%)	
I	41 (5.6)
II	101 (13.9)
III	315 (43.4)
IV	269 (37.1)
LRFS state,n (%)	
No	663(91.3)
Yes	63 (8.7)
DMFS state,n (%)	
No	638(87.9)
Yes	88(12.1)
PFS state,n (%)	

Characteristic	Overall
No	565 (77.8)
Yes	161 (22.2)
OS state,n (%)	
No	564 (89.7)
Yes	75(10.3)
Age,median(range)	47(11-78)
T-SUVmax, median(range)	8.89(2.51-48.88)
T-MTV, median(range)	12.71(0.77-131.01)
LDH, median(range)	166.5 (71-823)

Figures

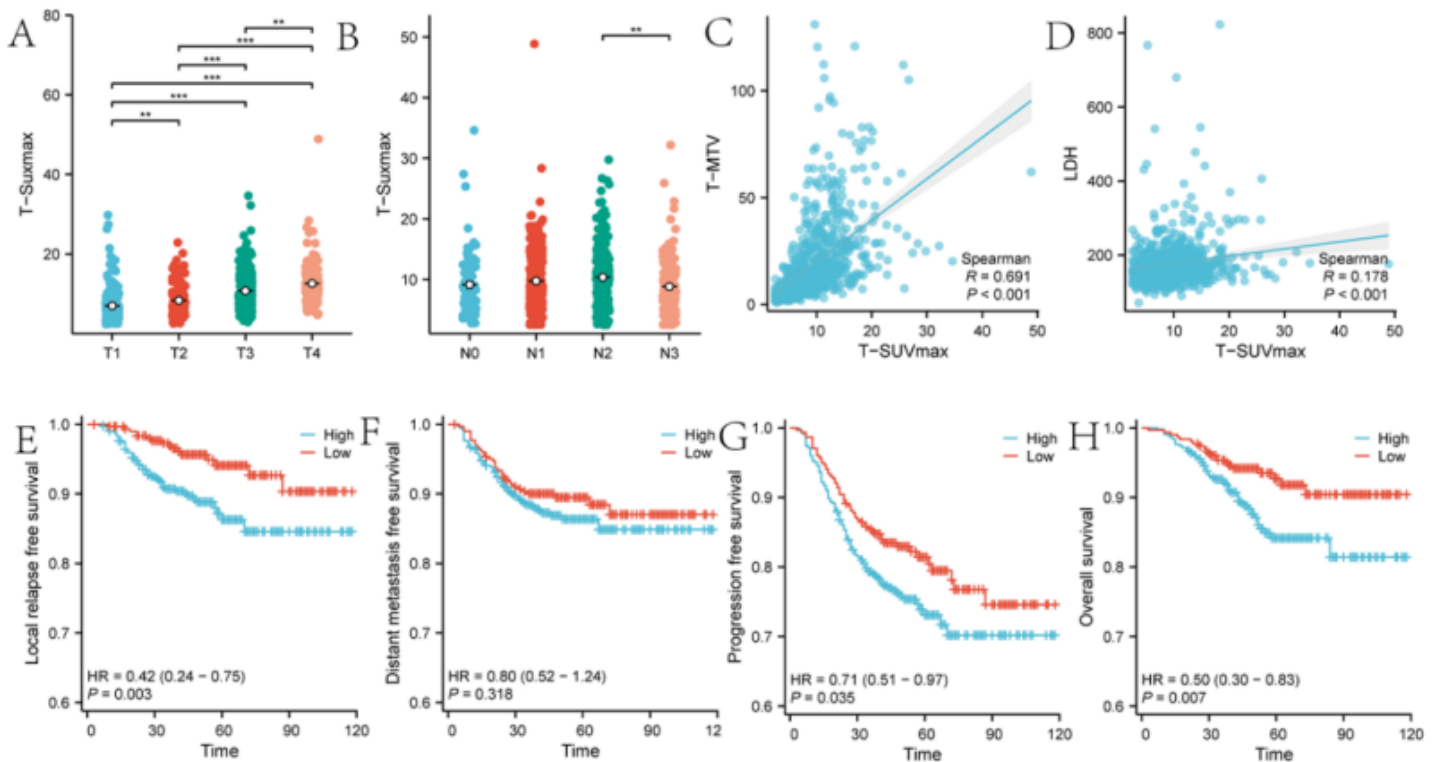


Figure 1

Suvmax Associations with Clinical Variables in Nasopharyngeal Carcinoma

(A and B) Boxplots illustrate the distribution of Suvmax across different T and N stages in NPC patients. (C and D) Scatter plots demonstrate the correlation of Suvmax with key parameters such as MTV and LDH. (E, F, G, and H) The figure presents survival curves for LRFS, DMFS, PFS, (and) OS, respectively.

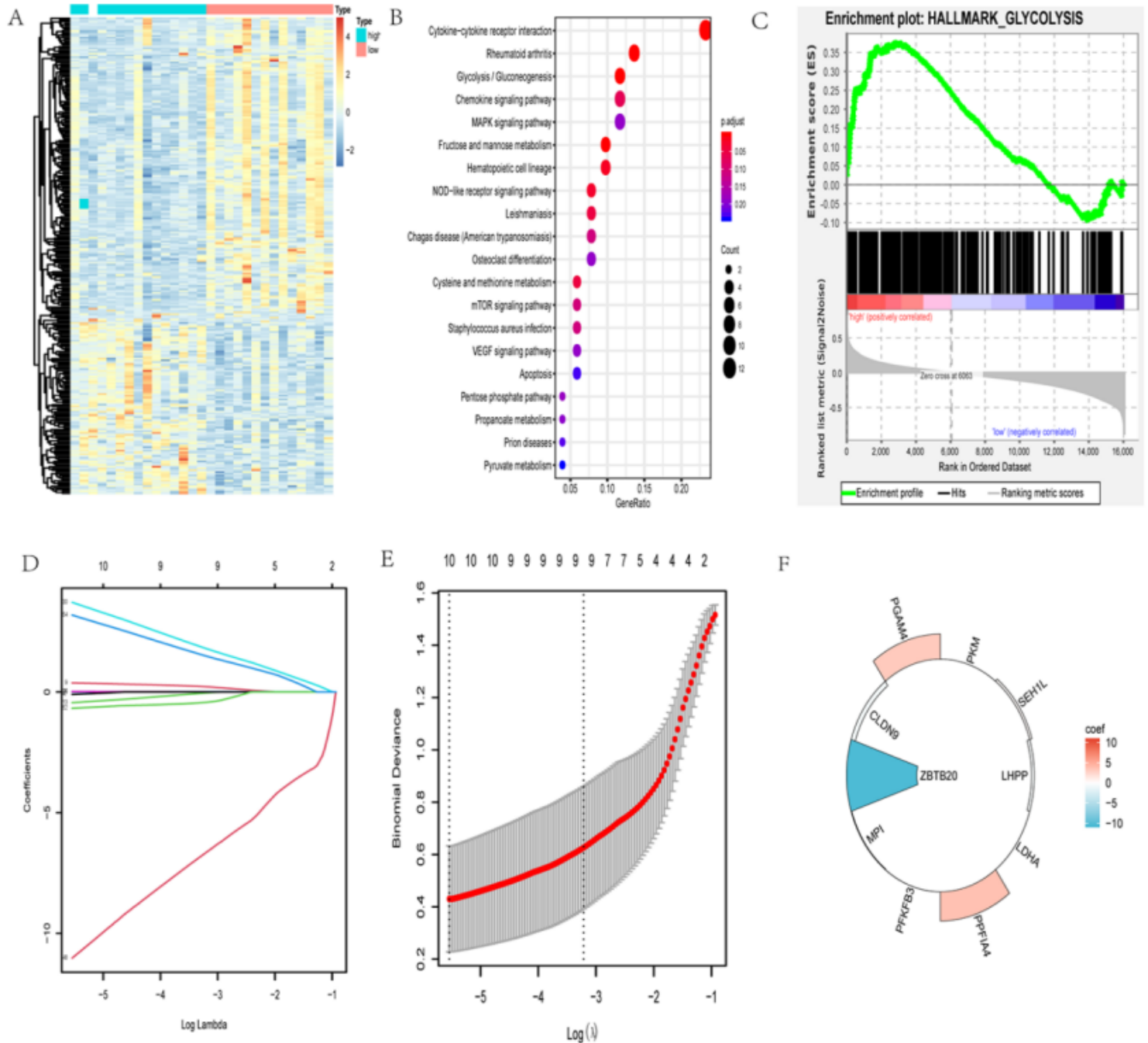


Figure 2

Suv-signature Building.

(A) Heatmap depicting differential gene expression between the high and low Suvmax groups. (B and C) GO enrichment analysis and GSEA conducted on the differentially expressed genes within the high and

low Suvmax groups.(D, E) Genes selected through LASSO regression and logistic analysis. (F) Contribution of the selected genes in constructing the Suv-signature along with their corresponding regression coefficients.

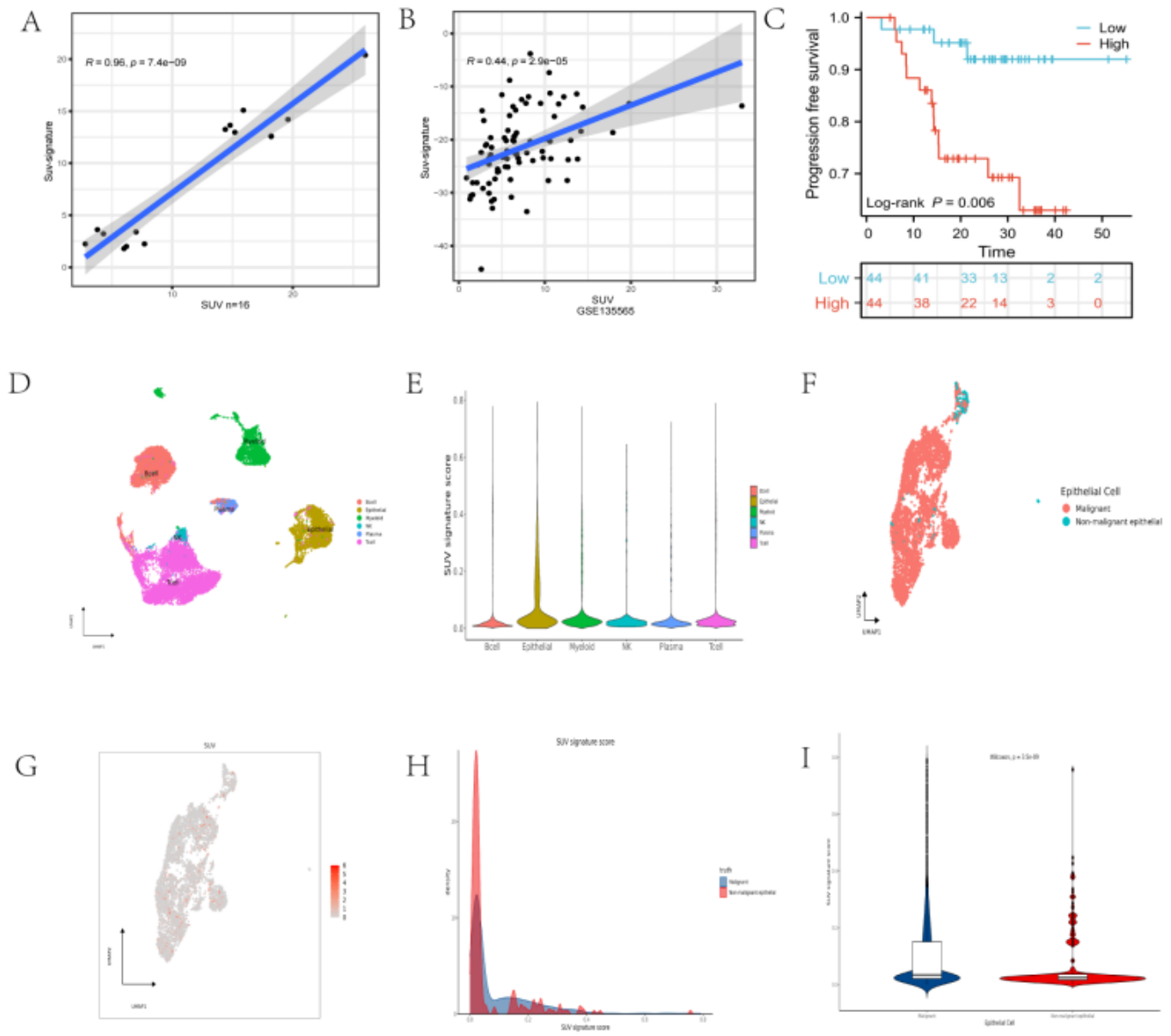


Figure 3

-signature Predicts Suvmax and Prognosis

(A,B) Association between Suv-signature and Suvmax in our 16 patient cohort and GSE135565.(C) Prognostic prediction by Suv-signature in GSE102349.(D) UMAP plot visualizing the clusters of each cell type in NPC.(E) Violin plot depicting the expression of Suv-signature score in each cell type.(F, G) UMAP plot illustrating the expression of Suv-signature in epithelial cells.(H, I) Density and Violin plot showing the expression of Suv-signature score in malignant epithelial cells and normal epithelial cells.

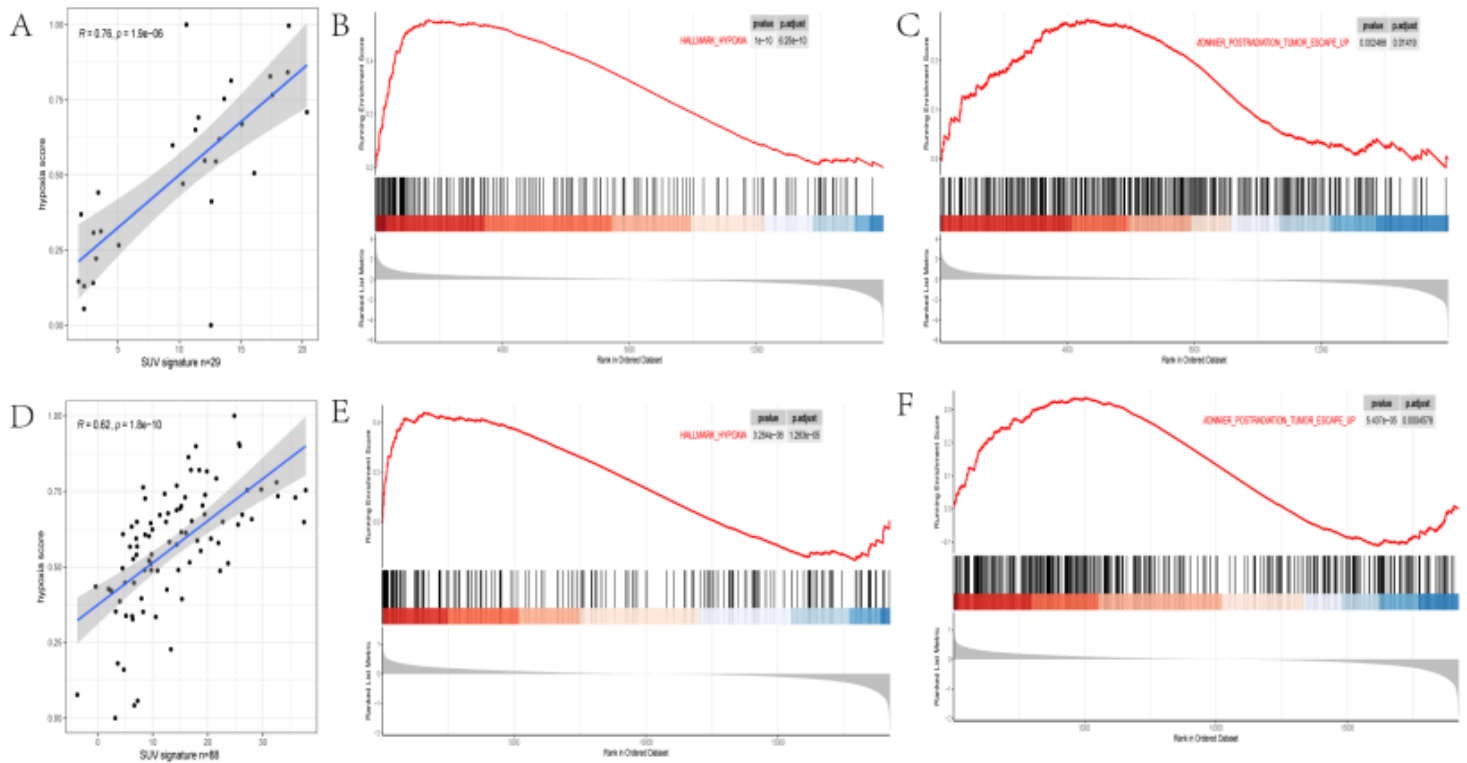


Figure 4

Suv-signature Association with Hypoxia and Radiotherapy Resistance

(A, D) Scatter plots illustrating the relationship between SUV-signature and hypoxic score in our center data and GSE102349.(B, C, E, and F) GSEA enrichment analysis conducted in our center data and GSE102349.

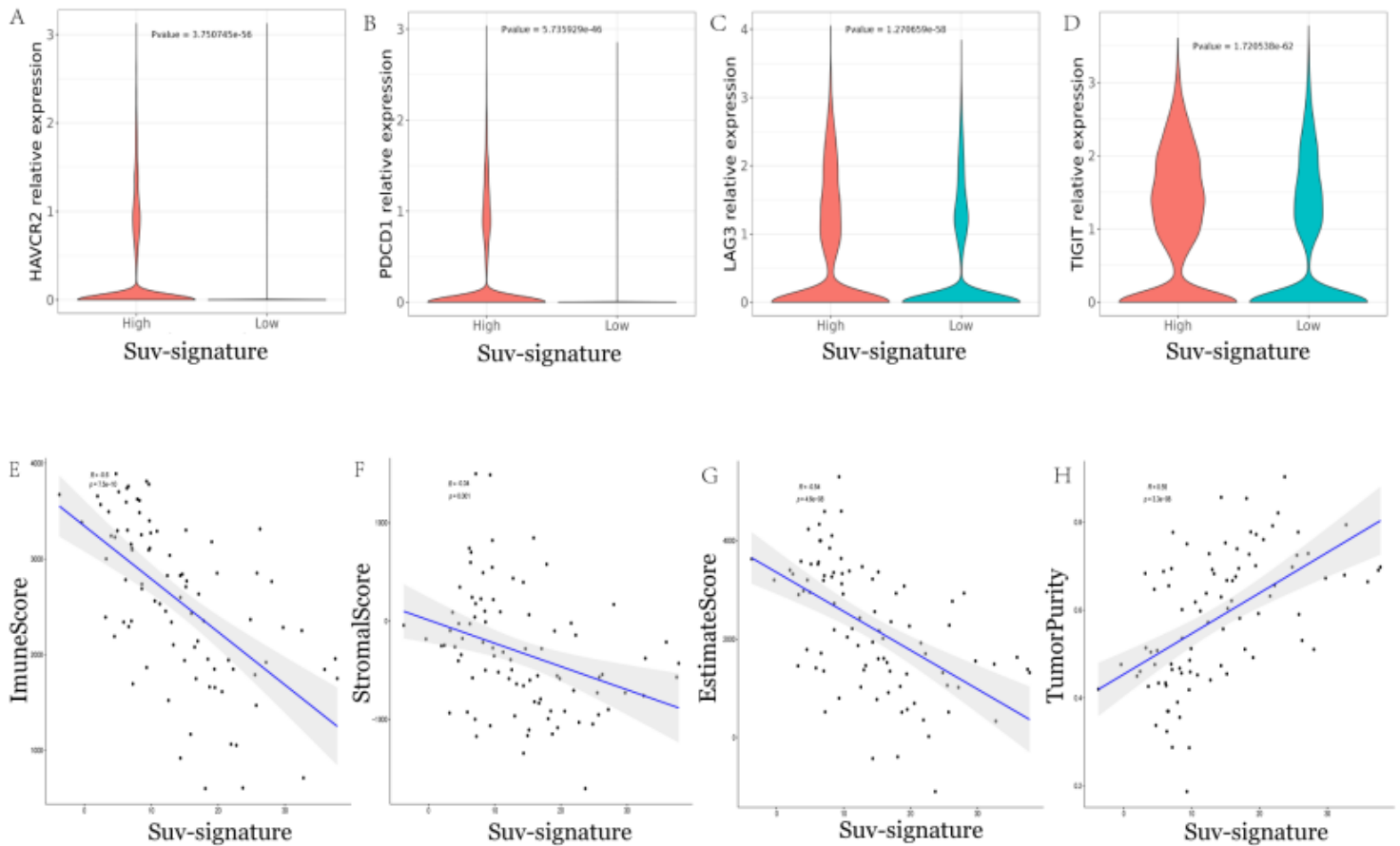


Figure 5

Relationship between SUV-signature and Immune Function

(A-D) Violin plots depict the expression levels of HAVCR2, PDCD1, LAG3, and TIGIT in T cells with high and low SUV-signature scores. (E-H) Illustrate the correlation between SUV-signature and immune score, stromal score, predictive score, and tumor purity.

Supplementary Files

This is a list of supplementary files associated with this preprint. Click to download.

- [Supplement.docx](#)